Vibration analysis of 3D printed PLA beam with honeycomb cell structure for renewable energy applications and sustainable solutions

Kubilay ASLANTAS[1,a*], Ekrem ÖZKAYA[2,b], Waleed AHMED[3,c,*]

[1] Department of Mechanical Engineering, Faculty of Technology, Afyon Kocatepe University, Afyonkarahisar, Turkey

[2] Faculty of Engineering - Department of Mechanical Engineering, Turkish-German University, 34820 Beykoz / İSTANBUL, Turkey

[2] Mechanical Engineering Department College of Engineering, UAE University, Al Ain, Abu Dhabi; UAE

[a]aslantas@aku.edu.tr, [b]ekrem.oezkaya@tau.edu.tr, [c]w.ahmed@uaeu.ac.ae

Keywords: Additive Manufacturing, Vibration Analysis, Finite Element Method

Abstract. Research shows a lack of vibration analyses of structures produced by 3D printing. This study, therefore, investigates the vibration behavior of honeycomb structures made of polylactic acid (PLA) using the additive manufacturing process fused deposition modeling (FDM) in a beam element. Based on an experimental modal analysis and the determination of the damping rate, a FEM reference simulation model is created, and the results are validated with the data from the experiment. The original honeycomb structure was numerically varied in its density, i.e., in the thickness (t) of the cell wall, in the length (L) of the regular hexagons, and in its degree of filling. The results showed that the density of the honeycombs at a filling level of 19% has a marginal influence on the vibration behavior. The vibration behavior was reduced only when the filling level was increased to 30%. This study has implications for many areas of research in which vibrations play a significant role in technical applications. These findings highlight the potential for integrating renewable energy applications with sustainable solutions, emphasizing the importance of vibration dynamics in advancing environmentally friendly technologies.

Introduction
Digital manufacturing technology, also known as 3D printing or additive manufacturing, has revolutionized the field of manufacturing. It allows for the production of complex structures with high precision and customization by successively adding materials based on three-dimensional computer-aided design (CAD) data [1]. Various techniques are available for 3D printing, with the most common being powder bed fusion (PBF) and fused deposition modeling (FDM) [2]. The ability to use various materials, including thermoplastics, ceramics, graphene-based materials, and metals, offers numerous application possibilities [3]. An overview of significant advances, typical applications, current challenges, advantages, and disadvantages of 3D printing processes, and a comprehensive description of various materials can be found in [4-5]. The use of plastics is becoming increasingly popular due to their excellent properties (high strength-to-mass ratio, low cost, durable, relatively impermeable, sterilizable) with controllable flexibility. In particular, there is growing interest in the use of biodegradable polymers. The most extensively investigated (bio)degradable thermoplastic polymers, which are also suitable for additive manufacturing technologies, are polyesters such as polylactic acid (PLA), polycaprolactone (PLC), and polyhydroxyalkanoates (PHA) [6]. Polylactic acid (PLA), a biodegradable and environmentally friendly thermoplastic, has emerged as a popular choice for 3D printing due to its ease of use and versatility [7]. The properties of PLA can also be chemically altered through synthesis or physical modifications [8-9]. The integration of honeycomb geometries into structural components has been

found to be applicable in many industries due to its potential to improve strength-to-weight ratios and overall mechanical efficiency [10]. However, the addition of internal honeycomb cell structures (which have good energy absorption properties) can add a layer of complexity to the material, influencing its dynamic response to external stimuli, especially vibrations. Geometric revisions to the extruded honeycomb structures will also significantly affect the vibration characteristics of the structure. The modal analysis technique is often used to determine the dynamic characterization of a structure or a machine element. Modal analysis determines a system's natural frequencies, mode shapes, and damping characteristics. The basic concept of modal analysis lies in representing the vibration response of a time-invariant linear dynamic system as a linear combination of a series of simple harmonic motions called natural modes of vibration. Modal analysis is an experimental approach that a hammer impact test or a vibration shaker can perform. Modal analysis of any structure or component must not be performed experimentally. When appropriate boundary conditions are defined, modal analysis can be performed using the finite element technique (FEM) to obtain the mode shapes and frequencies of the structure. With the widespread use of additive manufacturing in the last decade, porous structures' vibration-damping properties have been modeled experimentally and numerically. To increase the impact or vibration-damping properties of a structure, the pore structures shown in Figure 1 are widely used. Honeycomb geometry is frequently used in sandwich panels, and these structures' vibration behavior has been the subject of many studies [5].
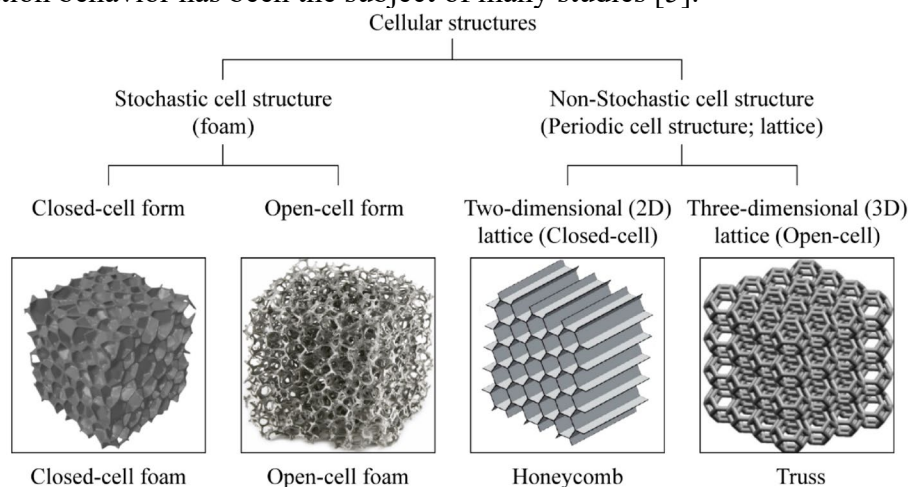

Fig. 1. Categories of cellular structures [12].

There is a lack of vibration analyses of structures produced using 3D printing in research. Understanding such structures' vibration characteristics is essential to ensure optimum performance in practical applications. This study investigates the effect of the honeycomb lattice structure on the vibration behaviour of a beam made of PLA material. In the study, firstly, a 3D printed PLA beam was produced by taking the edge length (L) and thickness (t) of the honeycomb lattice geometry as constant, and the damping ratio and resonant frequencies were found by performing a hammer test. The mode frequencies and vibration amplitudes obtained by numerical modeling are compared. FE analyses are extended for different values of L and t of the honeycomb geometry.

Material and Method
In the first stage of the study, a sample of PLA material was produced using the FDM method. The hammer test was performed on this sample, and the damping ratio of the material was determined. The damping ratio was used as input for harmonic analysis.

Sample Preparation

In this part of the study, the computer-aided design of the specified honeycomb geometry and the whole beam was carried out first. SpaceClaim software was used for the design. The 25 mm part of the beam (A region) is modeled as solid and is used to stabilize the beam (Fig. 2). The B region of the beam has a wall thickness of 0.75 mm and is filled with honeycomb. The dimensions of the honeycomb used are also given in Figure 2.
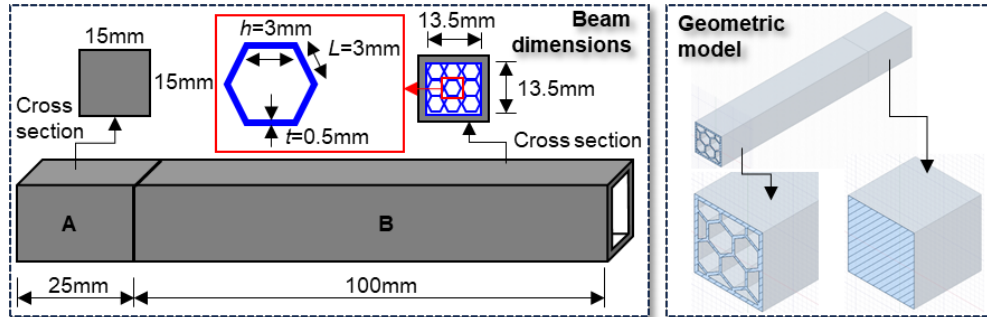

Fig.1. Dimensions and geometrical modeling of the beam

Experimental analysis

Figure 3 shows a schematic representation of the experimental procedure used in the study. The 3D-printed specimen was fixed from the A region (Fig. 2) employing a vice. An accelerometer was connected to the tooltip to measure the natural frequencies of the specimen. A Dytran brand hammer with model number 5800B4 was used for tap testing. A Dytran accelerometer (322F1) was mounted at the relevant position to measure the frequency response. A four-channel data acquisition system (Novian, model number S04) was used in conjunction with the Tap Testing measurement module of the CutPRO software to obtain the results of the vibration characteristics of the specimen. After the measurement, force-time, acceleration-time graphs and real-frequency and imaginary-frequency changes were obtained. In addition, the amplitude value occurring in the sample at the first mode frequency was also obtained. For numerical modeling, the damping ratio value of the sample must be known. The damping ratio of the sample was calculated using the real-frequency change obtained after the tap testing (Fig. 4).
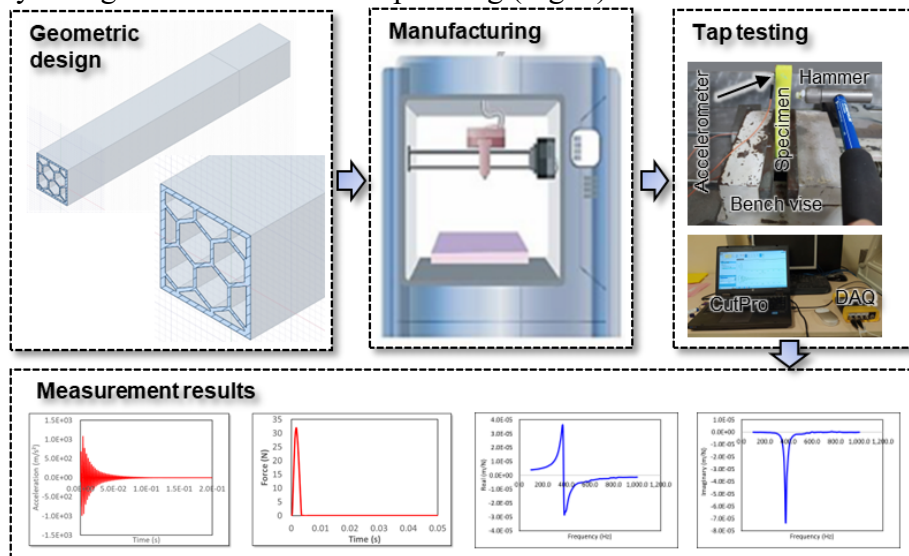

Fig. 3. Schematic representation of the experimental procedure used in the study

The specimen's real and imaginary part curves were obtained after the hammer test. The peak points (ω_1 and ω_2) in the real part curve and the values corresponding to the natural frequency (ω_n) were used. The damping ratio value of the specimen was calculated using Eq. 1.

$$\zeta = \frac{\omega_2 - \omega_1}{2.\,\omega_n} \tag{1}$$

Numerical modeling

Ansys software was used for FE analysis, and SpaceClaim software was preferred for geometric design. After the geometric model was imported to Ansys software [13], modal analysis was performed to find the mode frequencies. Afterward, the frequency response of the sample was obtained by performing harmonic analysis. In both analyses, part A of the specimen was fixed as anchored. In the harmonic analysis, the load was applied in the direction of the hammer load. Prior to numerical modeling, mesh convergence analysis was performed to determine the sufficient number of elements and nodes. Figure 5 shows the steps of the numerical modeling process used in the study. The modulus of elasticity of the PLA material used was taken as 2350 MPa, Poisson's ratio as 0.39, and density as 1.25 g/cm^3. In addition, the damping ratio was obtained as 0.022 using the method mentioned in the previous section. In the modeling, 31752 elements (tetrahedrons with 10 nodes) and 56764 nodes were used.
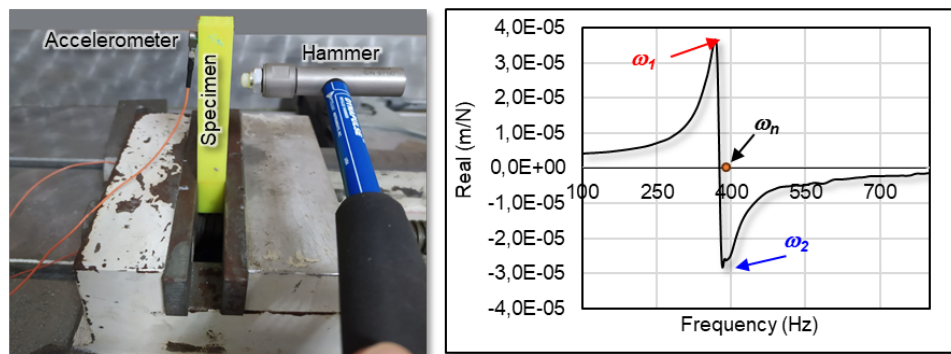

Fig. 4. Tap testing test setup and real part graph used to calculate the damping ratio.
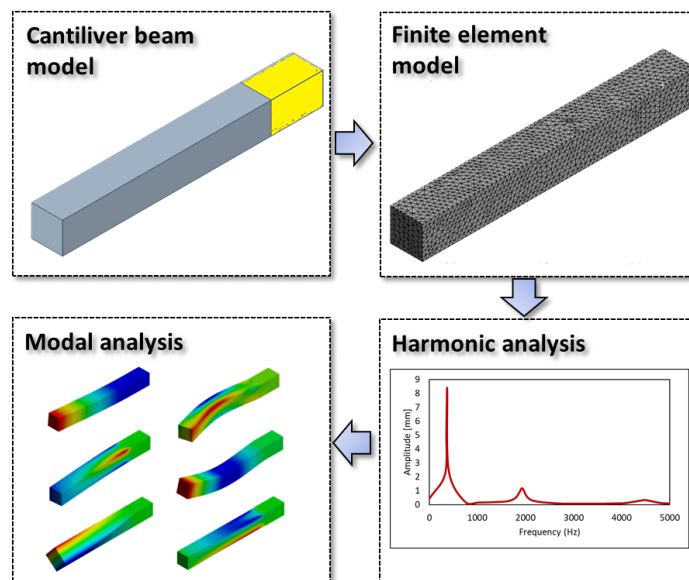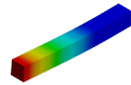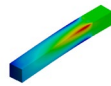

Fig. 5. Schematic representation of the steps used in numerical modeling
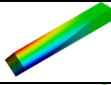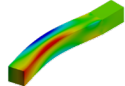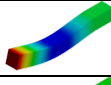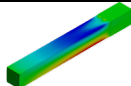
Results and Discussion

Tap testing results and verification of the FE model

In the study, experimental studies were first completed, and the value of the damping ratio required for numerical modeling was determined. Frequency values in each mode were obtained by hammer test. The frequency values for each mode obtained after numerical modeling were compared with the experimental results (Table 1). As can be seen from Table 1, there is a good agreement in the other frequency values except the 2nd mode value. The high margin of error in the 2nd mode frequency value may be due to two reasons. The first is that the point where the load is applied during the hammer test is not the same every time. The second is the minor dimensional errors caused during the production of the specimen. In particular, even slight differences in the wall thickness of the honeycomb may have caused this error.

Table 1. Comparison of experimental and numerical results and mode shapes

Mode No	Experimental	Modelling	Error (%)	Mode shape
1	363	364.8	0.5	
2	447.6	376.6	-18.8	
3	1687.9	1768.8	4.6	
4	1998.1	1952.4	-2.3	
5	2046.5	1986.1	-3	
6	3494.4	3435.5	-1.7	

After numerical modeling, the amplitude-frequency variation obtained for the 1st mode was compared with the experimental result (Fig. 6). As seen from Figure 6, the experimental and numerical modeling results agree very well. This shows the accuracy of the FE model and the boundary conditions used. It is seen that the maximum amplitude value occurs as 0.165 mm at 363 Hz in the experimental study, while it occurs as 0.166 mm at 364.8 Hz in the FE analysis.
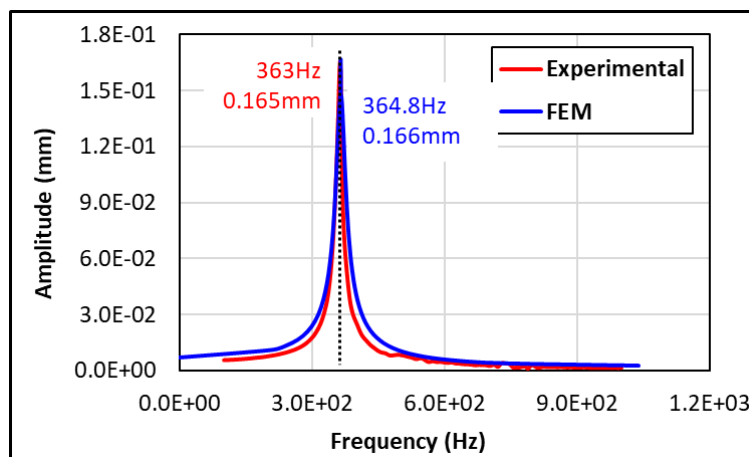

Fig. 6. Comparison of amplitude-frequency variation results in the beam

Vibration behavior of the revised honeycomb geometry

In the previous section, the vibration behavior of the honeycomb-filled PLA beam was obtained by hammer-impactor test, and the FE model was also validated. In this section, geometrical revisions were made to the honeycomb geometry, and the effects of the honeycomb's edge length, thickness, and filling rate were investigated. In lattice structures, changing the dimensions of the cell geometry causes a change in the filling rate. The FE analyses carried out in this section were performed for three different cell sizes, two different filling rates, and solid and hollow cases of the beam. Modal and then harmonic analyses were performed for the geometrical models. Thus, it was possible to calculate how much the revision in the honeycomb geometry affects the vibration amplitude and 1st mode frequency. Figure 7 shows different sections of the beam geometry used in the FE analysis. The effect of the change in cell edge length (L), cell edge thickness (t), and filling rate was investigated.
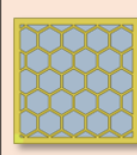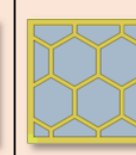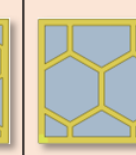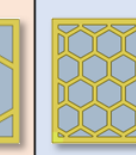
Filling rate (%)	100	---	19			30
Description	Solid beam	Hollow beam	L=1.5mm t=0.25mm	L=3mm t=0.5mm	L=4mm t=0.67mm	L=1.7mm t=0.5mm
Cross section						

Fig. 7. Cross sections of the beam geometry used in FE analysis

Figure 8 shows the amplitude-frequency variation obtained as a result of the harmonic analysis. Since the maximum amplitude occurs in the 1st mode in the beam, only 1st mode values are given in Figure 8. The hollow beam has the lowest stiffness among the analyzed sections. As expected, the maximum amplitude occurred in the hollow beam. All three sections' 1st mode frequency values with a filling rate of 19 are very close. In the inner graph in Figure 8, the graph for the % filling rate of 19% is detailed. As can be seen, the maximum amplitude was realized at L = 4 mm and t = 0.67 mm.

On the other hand, the maximum frequency was obtained for L = 1.5 mm and t = 0.25 mm. According to these three results, where the filling rate is constant, the variation of L and t does not affect the vibration amplitude and frequency much. When the filling rate ratios are compared, the amplitude value obtained for 30% is lower than 19%. On the other hand, the frequency value for 30% is lower than 19%. The amplitude value is minimum since the solid beam is the section geometry with the highest stiffness. However, the solid beam is the cross-section with the lowest 1st mode frequency value.
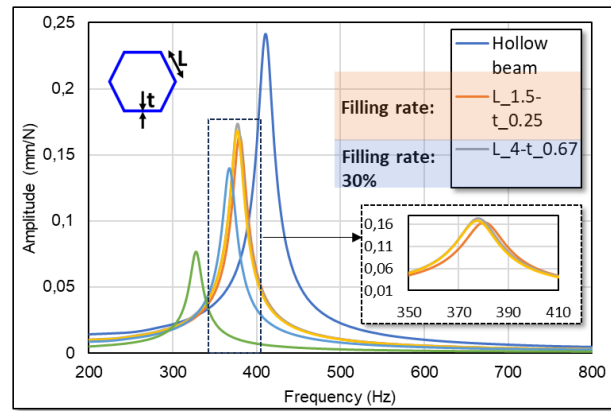
Fig. 8. Comparison of amplitude-frequency

Conclusion

This study thoroughly examined the impact of utilizing honeycomb geometry as a filling element within the beam structure. Experimental samples, crafted from PLA material with L=3 mm and t=0.5 mm (filling rate: 19%), were rigorously analyzed and validated through FE analysis. The validated FE simulation model enabled the exploration of varying densities (different L and t values) at 19% and 30% filling rates, shedding light on critical findings:

• The resonance frequency values obtained experimentally and numerically exhibited strong agreement, validating the reliability of the analysis.

• Maximal resonance amplitudes occurred at the 1st mode frequency, consistently verified through experimental and numerical approaches.

• Variations in L and t ratios, while holding the filling rate constant, minimally affected both amplitude and frequency.

• Increasing the filling rate resulted in decreased vibration amplitudes and frequencies, highlighting the role of density in vibration behavior.

The validated FE simulation model serves as a robust foundation for future investigations. Subsequent studies will explore diverse materials, filling structures, and structural densities while examining the influence of various pressure parameters. These efforts aim to advance sustainable practices and renewable energy applications, contributing to the ongoing evolution of environmentally conscious engineering solutions.

The research highlights the potential of 3D-printed honeycomb structures for renewable energy applications. Their vibration behavior, characterized through experimental analysis, offers opportunities for enhancing efficiency in energy harvesting devices and damping mechanisms. The structures' adaptability and lightweight nature make them suitable for components in wind turbines, solar panels, and energy storage systems. Integrating these structures into renewable energy technologies holds promise for advancing sustainable solutions and improving overall system performance.

References

[1] A. M. T. Syed, P. K. Elias, B. Amit, B. Susmita, O. Lisa, & C. Charitidis, "Additive manufacturing: scientific and technological challenges, market uptake and opportunities," Materials today, Vol. 1, pp. 1-16, 2017

[2] Shulman, H.; Spradling, D.; and Hoag, C.: Introduction to additive manufacturing, Ceram. Indus. 162:15-21, 2012.

[3] N. Shahrubudin, T.C. Lee, R. Ramlan, An Overview on 3D Printing Technology: Technological, Materials, and Applications, Procedia Manufacturing, Volume 35, 2019, Pages 1286-1296. https://doi.org/10.1016/j.promfg.2019.06.089

[4] Ji-chi Zhang, Kuai He, Da-wei Zhang, Ji-dong Dong, Bing Li, Yi-jie Liu, Guo-lin Gao, Zai-xing Jiang, Three-dimensional printing of energetic materials: A review, Energetic Materials Frontiers, Volume 3, Issue 2, 2022, Pages 97-108,7. https://doi.org/10.1016/j.enmf.2022.04.001

[5] Anketa Jandyal, Ikshita Chaturvedi, Ishika Wazir, Ankush Raina, Mir Irfan Ul Haq, 3D printing – A review of processes, materials and applications in industry 4.0, Sustainable Operations and Computers, Volume 3, 2022, Pages 33-42. https://doi.org/10.1016/j.susoc.2021.09.004

[6] Jennifer Gonzalez Ausejo, Joanna Rydz, Marta Musioł, Wanda Sikorska, Henryk Janeczek, Michał Sobota, Jakub Włodarczyk, Urszula Szeluga, Anna Hercog, Marek Kowalczuk, Three-dimensional printing of PLA and PLA/PHA dumbbell-shaped specimens of crisscross and transverse patterns as promising materials in emerging application areas: Prediction study, Polymer Degradation and Stability, Volume 156, 2018, Pages 100-110. https://doi.org/10.1016/j.polymdegradstab.2018.08.008

[7] Iftekar, S.F.; Aabid, A.; Amir, A.; Baig, M. Advancements and Limitations in 3D Printing Materials and Technologies: A Critical Review. *Polymers* **2023**, *15*, 2519. https://doi.org/10.3390/polym15112519

[8] Rasal RM, Janorkar AV, Hirt DE. Poly(lactic acid) modifications. Prog Polym Sci 2010;35:338-356. https://doi.org/10.1016/j.progpolymsci.2009.12.003

[9] Arrieta MP, López J, Hernández A, Rayón E. Ternary PLA-PHB-limonene blends intended for biodegradable food packaging applications. Eur Polym J 2014;50:255-270. https://doi.org/10.1016/j.eurpolymj.2013.11.009

[10] Hossein Mohammadi, Zaini Ahmad, Michal Petrů, Saiful Amri Mazlan, Mohd Aidy Faizal Johari, Hossein Hatami, Seyed Saeid Rahimian Koloor, An insight from nature: honeycomb pattern in advanced structural design for impact energy absorption, Journal of Materials Research and Technology, Volume 22, 2023, Pages 2862-2887. https://doi.org/10.1016/j.jmrt.2022.12.063

[11] Zippo, A.; Iarriccio, G.; Pellicano, F.; Shmatko, T. Vibrations of Plates with Complex Shape: Experimental Modal Analysis, Finite Element Method, and R-Functions Method. *Shock. Vib.* **2020**, 8882867. https://doi.org/10.1155/2020/8882867

[12] Park, K.-M.; Min, K.-S.; Roh, Y.-S. Design Optimization of Lattice Structures under Compression: Study of Unit Cell Types and Cell Arrangements. *Materials* **2022**, *15*, 97. https://doi.org/10.3390/ma15010097

[13] ANSYS Inc. (2022). ANSYS Software. Retrieved from https://www.ansys.com